

# Critical Fluctuations in Plasma Membrane Vesicles

Sarah L. Veatch<sup>†,\*</sup>, Pietro Cicuta<sup>‡</sup>, Prabuddha Sengupta<sup>†</sup>, Aurelia Honerkamp-Smith<sup>§</sup>, David Holowka<sup>†</sup>, and Barbara Baird<sup>†</sup>

<sup>†</sup>Department of Chemistry and Chemical Biology, Cornell University, Ithaca, New York 14853, <sup>‡</sup>Cavendish Laboratory University of Cambridge, Cambridge, UK CB30HE, and <sup>§</sup>Department of Chemistry, University of Washington, Seattle, Washington 98195

It is generally acknowledged that plasma membrane lipids contribute to cellular processes, although very little is known regarding the underlying physical basis by which lipids accomplish this function. A current and popular hypothesis is that cellular plasma membranes contain dynamic sub-micrometer “raft” domains that are enriched in certain lipid and protein species, and that these rafts can change in size, composition, and stability in response to environmental cues (1–4). It is often speculated that this raft organization arises from the tendency for lipids in membranes containing cholesterol to separate into coexisting liquid-ordered ( $L_o$ ) and liquid-disordered ( $L_d$ ) phases. Indeed, there are now numerous experimental observations of plasma membrane lipids existing in more ordered and less ordered states both in intact cells and in isolated or extracted membrane vesicles (5–10). While it is appealing to speculate that raft domains arise from phase separation, current descriptions of raft organization do not resemble phase-separated domains in model membranes. This lack of a clear physical basis of raft formation has complicated efforts to decipher the functional consequences of lipid-mediated lateral organization in biomembranes.

Critical points are special compositions and temperatures in the phase diagram where tie-lines merge into single points and where the compositions of coexisting phases become identical. In multicompo-

nent systems, the “osmotic compressibility” diverges at the critical point, meaning that very little energy is required to maintain regions of inhomogeneous composition. This divergence leads to a wide range of critical phenomena that are well-understood in terms of both theory and experiment (11, 12). When a critical point is approached from within the two-phase coexistence region, the increasing osmotic compressibility acts to reduce the interfacial energy between phases, and thermal energy drives elongation and roughening of domain boundaries (13). When a critical point is approached from the one-phase region, the increasing osmotic compressibility allows for the formation of long-range composition fluctuations. The composition of these fluctuations mirrors the underlying tie lines, and their size and lifetime increase and ultimately diverge as the critical point is approached (12). Importantly, many aspects of critical behavior are universal, meaning that they apply to all systems independent of the specific interactions that give rise to the presence of the critical point. The 2D Ising model is a two-state model with nearest neighbor interactions that has been solved exactly (14) and has been used to successfully describe the behavior of a wide range of experimental systems near critical points, including spin magnets (15), liquid crystals (16), and multicomponent mixtures that give rise to two liquid phases (12). We recently observed critical fluctuations in model membranes containing cholesterol

**ABSTRACT** We demonstrate critical behavior in giant plasma membrane vesicles (GPMVs) that are isolated directly from living cells. GPMVs contain two liquid phases at low temperatures and one liquid phase at high temperatures and exhibit transition temperatures in the range of 15 to 25 °C. In the two-phase region, line tensions linearly approach zero as temperature is increased to the transition. In the one-phase region, micrometer-scale composition fluctuations occur and become increasingly large and long-lived as temperature is decreased to the transition. These results indicate proximity to a critical point and are quantitatively consistent with established theory. Our observations of robust critical fluctuations suggest that the compositions of mammalian plasma membranes are tuned to reside near a miscibility critical point and that heterogeneity corresponding to <50 nm-sized compositional fluctuations are present in GPMV membranes at physiological temperatures. Our results provide new insights for plasma membrane heterogeneity that may be related to functional lipid raft domains in live cells.

\*Corresponding author, sv232@cornell.edu.

Received for review January 16, 2008 and accepted March 6, 2008.

Published online May 16, 2008

10.1021/cb800012x CCC: \$40.75

© 2008 American Chemical Society

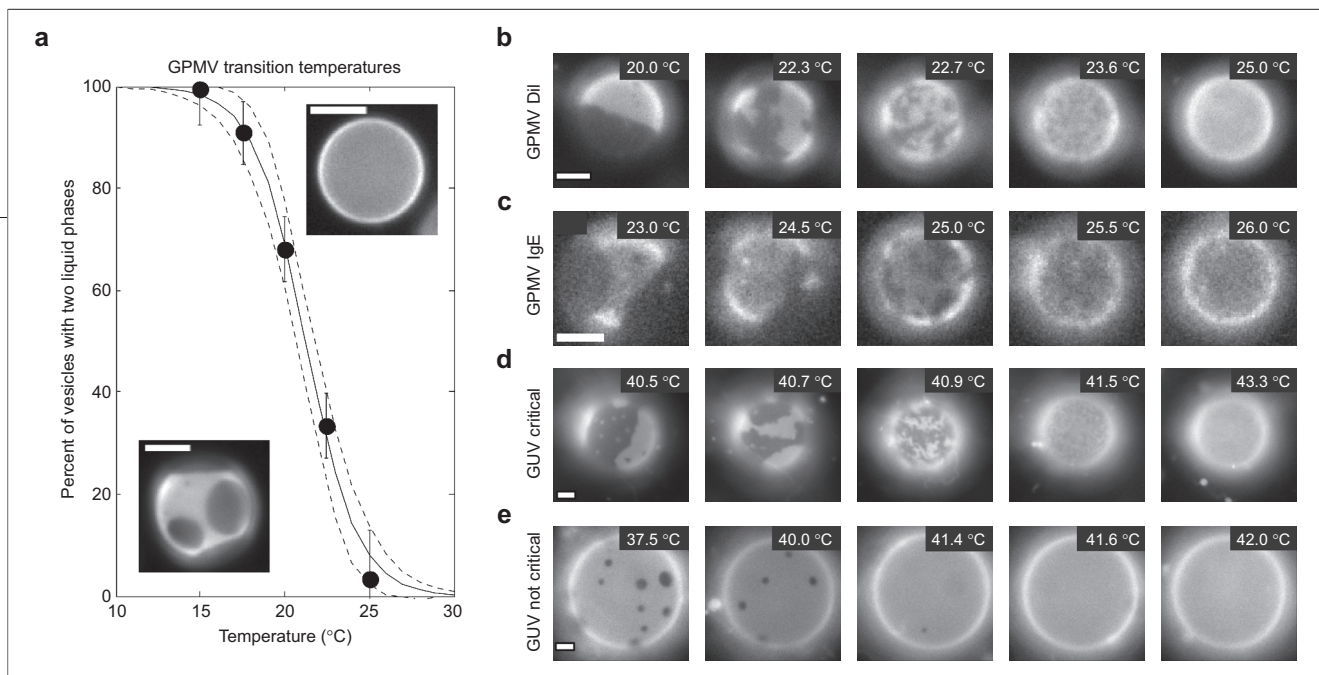


**Figure 1. Transition temperatures and critical fluctuations in GPMVs.** a) GPMVs from the same preparation show a distribution of miscibility transition temperatures, indicating that GPMVs have a distribution of membrane compositions (35). GPMVs are uniform at high temperature and contain two coexisting liquid phases at low temperature. Images shown were acquired at 25 and 15 °C, respectively, scale bars are 5  $\mu\text{m}$ , and error bounds denote Poisson ( $100/N^{1/2}$ ) counting statistics. b, c) Despite the inherent variation in transition temperature, all GPMVs undergo micrometer-scale fluctuations at temperatures just above their respective miscibility transition temperature, visualized when cells are prelabeled with a fluorescent lipid analog (panel b, DiIc12) or a fluorescently tagged antibody (panel c, Alexa488-IgE bound to Fc $\epsilon$ RI) (also see Supplementary Movies S1–S6). d) GPMVs closely resemble GUVs made from synthetic mixtures of phospholipids and cholesterol (Chol) prepared with near-critical lipid compositions (a vesicle of 1:1:2 diphyanoylphosphatidylcholine (diphyanoylPC)/dipalmitoylphosphatidylcholine (DPPC)/Chol with 0.5% DiIc12 is shown here). The critical temperature falls roughly between the second and third images in panels b–d. e) Fluctuations are not observed in GUVs prepared with a composition that does not pass through a critical point (2:2:1 diphyanoylPC/DPPC/Chol shown here.) Scale bars are 5  $\mu\text{m}$ .

and found that fluctuations are consistent with 2D Ising model scaling laws (17, 18).

## RESULTS AND DISCUSSION

GPMVs (giant plasma membrane vesicles) form as blebs directly from the plasma membranes of living rat basophil leukemia (RBL) cells after chemical treatment (8). These vesicles pull away from the cytoskeleton, and they contain a wide assortment of plasma membrane protein and lipid species. GPMVs undergo a miscibility transition; they appear to be made up of a single liquid phase at high temperatures and separate into two coexisting liquid phases below a miscibility transition temperature,  $T_{\text{mix}}$ . In any given GPMV preparation, we find a broad distribution of  $T_{\text{mix}}$  values when vesicles are viewed on a temperature-controlled microscope stage, usually in the range of 20 °C and spanning 5–10 °C (Figure 1, panel a). Mean transition temperatures can depend on numerous factors including the growth density of parental cells, vesiculation temperature, and perturbation of GPMVs with amphipathic molecules such as short chain ceramides (data not shown).

Remarkably, in over 100 GPMVs examined, we find that all GPMVs undergo domain boundary fluctuations below  $T_{\text{mix}}$  and micrometer-scale lateral composition fluctuations above  $T_{\text{mix}}$  (Figure 1, panels b and c and Supplementary Movies S1–S6). Several degrees below  $T_{\text{mix}}$ , GPMVs contain roughly equal area fractions of coexisting phases. Our observations of fluctuations are qualitatively consistent with all GPMVs having near-critical compositions despite the inherent variation in transition temperature between GPMVs in a single preparation. Critical behavior is visualized in GPMVs prelabeled with either fluorescent lipid analogs (DiIc12; Figure 1, panel b and Supplementary Movies S1 and S2) or with fluorescently tagged antibodies to membrane bound proteins (IgE bound to Fc $\epsilon$ RI (Figure 1, panel c and Supplementary Movie S3) or antibodies to Thy-1 (Supplementary Movie S4), indicating that both lipids and membrane bound proteins experience critical behavior. In most cases, this critical behavior is reversible, meaning that the same transition temperature and fluctuations are

observed with both increasing and decreasing temperature. This suggests either that photodegradation of lipids is not occurring in these membranes or that this degradation does not alter membrane phase behavior. Finally, we observe critical behavior in GPMVs derived from other cell types (NIH-3T3 and HEK, Supplementary Movies S5 and S6)). In all cases, the observed critical behavior closely resembles that found in giant unilamellar vesicles (GUVs) prepared with a lipid composition carefully chosen to reside near a miscibility critical point (Figure 1, panel d) and does not resemble GUVs prepared with compositions that pass through the miscibility transition temperature away from a critical point (Figure 1, panel e and Supplementary Movie S7).

Observations of robust critical fluctuations in GPMVs are remarkable because they suggest that cell plasma membranes, as represented by these vesicular membranes, have compositions that are tuned to reside near miscibility critical points, meaning that the miscibility transition temperature is also the critical temperature in

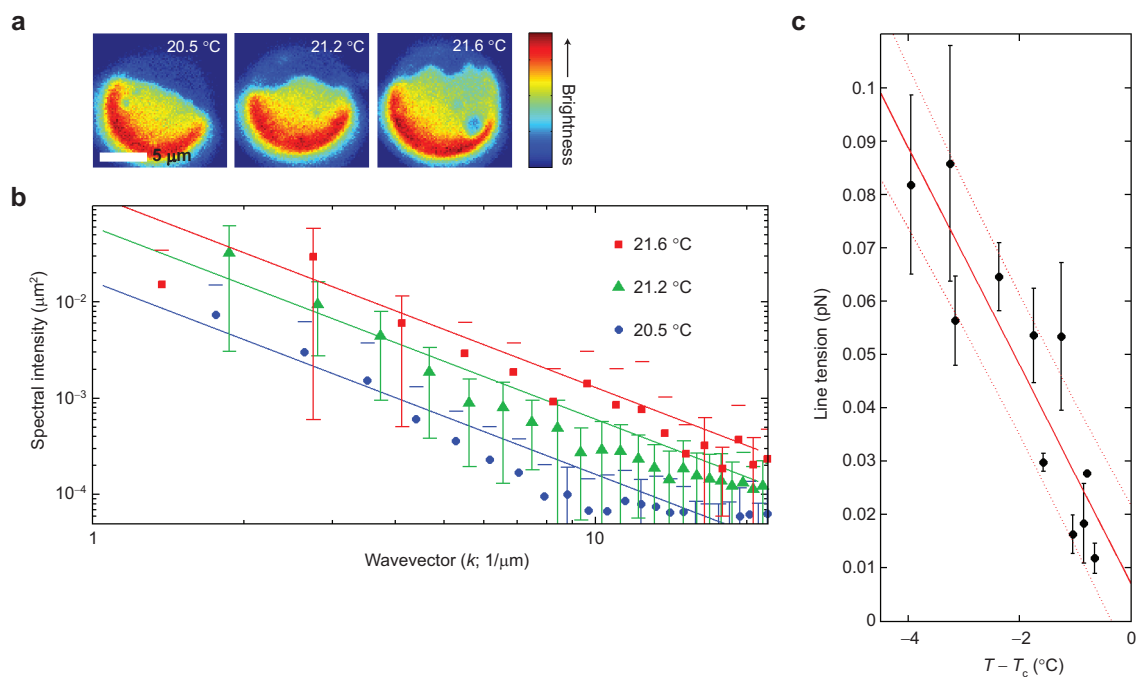


**Figure 2. Line tension measurements below the transition temperature indicating that GPMVs have critical compositions.** **a)** Pseudocolor images of phase-separated GPMVs below the transition temperature demonstrate that boundary fluctuations increase in magnitude as temperature is increased towards the transition temperature. **(b)** Line tensions are evaluated from the power spectrum boundary fluctuations as described in Materials and Methods. **(c)** Line tensions trend linearly to zero (within error) as the transition temperature is approached, consistent with predictions of the 2D Ising model. This indicates that membranes have critical compositions and that the transition temperature is the critical temperature.

these membranes. Furthermore, the fact that we observe critical behavior in all GPMVs, even though we find a broad distribution of transition temperatures, suggests that there is a distribution of closely spaced critical points in the many dimensional compositional space occupied by these complex biomembranes. In simple three-component model membranes, detailed knowledge of the phase diagram is required to find lipid compositions close enough to critical points to observe micrometer-scale critical fluctuations (17, 18). Thermodynamic rules stipulate that critical points are equally rare in randomly assembled symmetric model membranes with a greater number of components. It is tempting to conclude that the broad diversity and careful regulation of plasma membrane compo-

nents occurs, at least in part, to maintain cell plasma membranes in close proximity to miscibility critical points.

In the 2D Ising model, the line tension,  $\lambda$ , is a linear function of temperature,  $T$ , and intersects zero at the critical point, such that  $\lambda \approx \lambda_0(T_c - T)/T_c$ , where  $T_c$  is the critical temperature in units of kelvin (13). Line tensions are extracted from GPMV images by fitting the power spectrum of boundary fluctuations, as described in Materials and Methods (outlined in Figure 2). At temperatures well below the critical point, the phase boundary contour does not deviate significantly from the time-averaged value indicating that the line tension is large. As temperature approaches the transition, the magnitude of fluctuations increase, indicating that line tension is decreased. Plots of

line tension vs increasing temperature are well fit by a straight line, indicating good quantitative agreement with the 2D Ising model. When membranes pass through the phase boundary away from a critical point, line tension is expected to fall to a finite value at the transition temperature. We observe that measured line tensions fall to zero within error bounds at the transition temperature, as is expected when membranes pass through a critical point at the transition temperature, providing further evidence that the GPMV membranes contain critical compositions.

An independent quantitative analysis of critical behavior is conducted by analyzing composition fluctuations above the transition temperature (Figure 3). First, we examine the lateral distribution of fluorescent in-

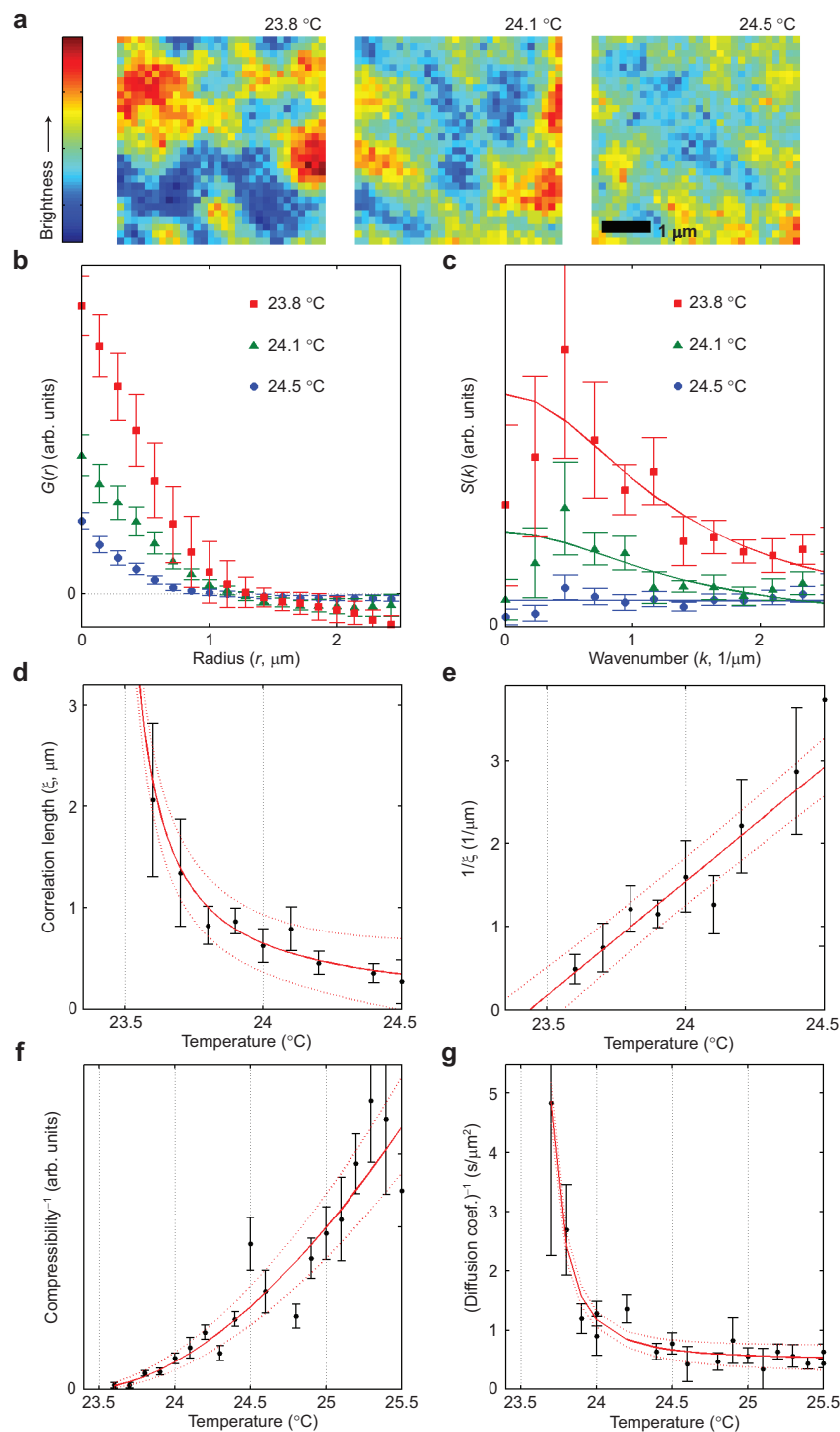


**Figure 3.** Critical fluctuations in GPMVs are quantitatively consistent with results of the 2D Ising model as depicted for a representative GPMV. **a)** Critical fluctuations are visible on the GPMV surface in pseudocolor images at the temperatures shown. **b, c)** Quantification of critical fluctuations is accomplished by computing the radially averaged autocorrelation function,  $G(r)$ , and its Fourier transform  $S(k)$ , where  $r$  is radius and  $k$  is the magnitude of the wavevector. The  $G(r)$  and  $S(k)$  traces shown are computed by averaging functions obtained from 10 images acquired at the temperatures shown. Error bars represent standard deviations over averaged values. **d)** Correlation lengths ( $\xi$ ) are extracted from  $S(k)$  curves and are plotted vs temperature ( $T$ ). **e)** Plots of  $1/\xi$  vs  $T$  are well fit by a straight line, which intersects the temperature axis at the critical temperature ( $T_c$ ), demonstrating agreement with the 2D Ising model. **f)** The extrapolated value of  $S(k=0)$  is proportional to the osmotic compressibility (black points) and diverges as  $(T_c/(T - T_c))^{7/4}$  (red line) as the critical temperature is approached. **g)** A time-dependent analysis of the inverse gradient diffusion coefficient ( $D^{-1}$ ) reveals correlation times that are consistent with 2D Ising model predictions (21). The red line goes as  $D^{-1} = A(T_c/(T - T_c))^2 + D_0^{-1}$ , where  $A$  is a proportionality factor and  $D_0$  is in good agreement with values expected for normal lipid diffusion. In all cases, the red line shows the best fit to the black data points, and the dotted line denotes  $\pm 1\sigma$  confidence intervals.

tensity on the vesicle surface at fixed time to determine the correlation length and the osmotic compressibility. These values are determined by evaluating the density–density correlation function,  $G(r)$ , which is a function of radius,  $r$ , and is defined as the radial average of the 2D autocorrelation of an image (11, 12) (Figure 3, panel b). When calculating  $G(r)$ , we assume that probe intensity is proportional to probe concentration (density), which is the order parameter measured (19). As with all optical microscopy measurements,  $G(r)$  curves are distorted by the point spread function of the microscope. We therefore found it easiest to perform our analysis using the structure factor,  $S(k)$ , which is the Fourier transform of  $G(r)$ , where  $k$  is the magnitude of the wavevector (see Materials and Methods).  $S(k)$  describes the spatial frequency distribution of composition fluctuations (Figure 3, panel d) and is often directly measured in three-dimensional systems through scattering experiments (12). The correlation length,  $\xi$ , reports the size of fluctuations and can be determined by fitting  $S(k)$  as described in Materials and Methods.

The 2D Ising model predicts that the correlation length varies inversely with the temperature distance from the critical point such that  $\xi \approx \xi_0 T_c / (T - T_c)$ . We find that plots of  $1/\xi$  vs temperature are well-fit by a straight line, the x intercept being a precise assignment of the critical temperature (Figure 3, panel e). The osmotic compressibility,  $\chi$ , is proportional to the zero frequency component of the structure factor,  $\chi \approx S(k=0)$  (11), and we find that it is well-fit by  $\chi \approx (T_c / (T - T_c))^{7/4}$ , also in agreement with predictions of the 2D Ising model for mixtures with critical compositions (11) (Figure 3, panel f). We have conducted an identical analysis on multiple GPMVs (>5) and obtained similar results.

We also investigated the time-dependence of critical fluctuations in GPMVs. Correlation times are expected to increase in membranes near a critical point,

meaning that membrane heterogeneity changes slowly (20). This occurs because there is little driving force to smooth out composition gradients in near-critical membranes, where only small energies are required to maintain regions of inhomogeneous compositions. In order to quantify this, we have evaluated inverse gradient diffusion coefficients,  $D^{-1}$ , as described in Materials and Methods.  $D^{-1}$  is a measurement of the time it takes for probes to diffuse over a specified area. We find that  $D^{-1}$  becomes large near the critical temperature, in a manner consistent with predictions of the 2D Ising model ( $D^{-1} \approx \xi^z$ , where  $z \approx 2$ ) (21). At high temperatures,  $D^{-1}$  drops to the finite value  $D_0^{-1}$ , which corresponds to a measurement of fluctuation lifetime limited by normal lipid diffusion. In this case, we find  $D_0^{-1} = 0.5 \pm 0.2 \text{ s}/\mu\text{m}^2$ , corresponding to a diffusion constant of  $D_0 = 2 \pm 1 \mu\text{m}^2/\text{s}$ , which is in general agreement with expected values for lipid diffusion in bilayer membranes (22, 23).

The quantitative agreement of our findings with those predicted by the 2D Ising model give us confidence to extrapolate our correlation length results to physiological temperatures, where the corresponding correlation lengths are inaccessible to the optical resolution of fluorescence microscopy measurements. As described above, we confirmed that correlation length goes as  $\xi \approx \xi_0 T_c / (T - T_c)$  (Figure 3, panel e). Our measured value of  $\xi$  is  $1 \mu\text{m}$  at  $\sim 0.3 \text{ }^\circ\text{C}$  above the critical temperature of  $23.4 \text{ }^\circ\text{C}$ ; therefore we expect to find a correlation length of  $1 \mu\text{m} \times 0.3/13.6 = 22 \text{ nm}$  in these GPMVs at physiological temperatures of  $37 \text{ }^\circ\text{C}$ . This length scale is comparable to recently proposed sizes of putative “raft” domains in resting cells (2–4) and suggests a possible physical basis for submicrometer lateral organization in the plasma membrane of intact cells.

While GPMVs capture much of the compositional complexity of intact plasma membranes, they differ in some fundamental as-

pects that still need to be explored. For example, GPMVs exclude membrane proteins attached to cytoskeletal components (24), there is some loss of asymmetry between membrane leaflets (8), and these membranes are no longer connected to active processes within the cell (e.g., lipid recycling). These are all factors predicted to modulate the phase behavior of membrane lipids (25–27) and likely contribute to the fact that macroscopic phase separation is not routinely observed in living cells at low temperatures. Even so, it is intriguing to speculate that lateral heterogeneities in living cells at physiological conditions correspond to critical fluctuations. In principle, perturbations that alter the phase boundary (and therefore the critical point) could have a large effect on the size, composition, and lifetime of critical fluctuations at physiological temperatures (28, 29). It has recently been shown that cross-linking components, an action often associated with cell activation, can alter phase transition temperatures in model membranes (30, 31). Alternatively, cells may simply exploit the low-energy cost associated with organizing membrane components in membranes with critical compositions. Our results point to critical behavior as an intriguing possibility for the physical basis of membrane lateral heterogeneity, and they provide motivation for further studies that probe the presence and functional relevance of critical fluctuations in intact cells.

## MATERIALS AND METHODS

**Experimental Procedures.** RBL cells were pre-labeled with either DiI12 or fluorescently tagged antibodies. GPMVs were prepared as described previously (8) and viewed between sealed coverslips using a Leica DM-IRB inverted microscope (Bannockburn, IL) with a  $40\times$ , 0.65 NA air objective coupled to a cooled CCD camera (Quantix, Photometrics, Tucson, AZ). In this configuration, the pixel size is  $143 \text{ nm}$ . Images were acquired every  $0.5 \text{ s}$  with  $250 \text{ ms}$  integration times for DiI measurements. Total DiI12 concentrations are estimated to be  $<0.25 \text{ mol } \%$  through comparison with GUV measurements. Temperature was controlled at the sample to better than  $0.05 \text{ }^\circ\text{C}$  using a Peltier-based microscope stage in combination

with a proportional–integral–derivative (PID) controller. Temperature was allowed to equilibrate between 1 and 5 min between image acquisitions depending on the magnitude of the temperature step. All analyses were conducted in Matlab.

**Line Tension Analysis ( $T < T_c$ ).** Line tensions are extracted by measuring the spatial frequency spectrum of boundary deviations from the time-averaged boundary as a function of temperature, as reported previously (32–34). To maximize sensitivity, we performed our measurements on vesicles that were completely phase separated, such that only a single boundary (a straight equatorial line on time average) was visible in the 2D projection of the membrane surface. The displacement of the boundary location from the time-averaged boundary,  $h(x)$ , was measured for each frame. We then performed a Fourier transform (FT) to obtain the frequency distribution of boundary fluctuations,  $h(k)$ , where the FT is defined as  $h(k) = 1/(2\pi) \int_{-\infty}^{\infty} dx h(x) e^{ikx}$ . The low wavenumber values of  $\langle h(k)^2 \rangle$ , excluding the  $k = 0$  value, were fit using linear regression to  $k_B T / (\lambda k^2)$ , to extract line tensions ( $\lambda$ ). Measured values of  $\lambda$  are in good agreement with previous studies employing similar analytical techniques (18, 34). Errors were either determined directly from the covariance matrix at the best fit solution or as a standard deviation over values when multiple vesicles examined at the same temperature distance from the critical point ( $T - T_c$ ).

**Critical Fluctuation Analysis ( $T > T_c$ ).** A geometrical correction is applied to images to account for the spherical nature of the vesicle surface as described in Supplementary Figure S1. Finite size 2D autocorrelations are determined using a 2D FT on the acquired image ( $I$ ) such that  $G(r, \theta) = \text{FT}^{-1}(|\text{FT}(I)|^2)$ , where  $G(r)$  is the density–density correlation function of the image. Before processing, acquired images were padded with zeros to eliminate periodic boundary conditions, and autocorrelation values were normalized to account for the variable number of pairs that contributed to each point,  $N(r, \theta)$ . Because few pairs contribute to large  $r$  values, these points have large associated errors. To account for this  $G(r, \theta)$  images are windowed by  $N(r, \theta)^{1/2}$  in order to reduce noise at large  $r$  when performing the FT to obtain  $S(k, \theta)$ . Structure factors were then radially averaged to obtain  $S(k)$ .

In our measurements, we find that camera resolution is better than the optical resolution, and as a result the acquired images appear to be “filtered” by the point spread function of the microscope. In real space, filtering is equivalent to performing a convolution of the filter with the original image. A convolution in real space is equivalent to a multiplication in Fourier (frequency) space; therefore correlation lengths and compressibilities were evaluated from corrected  $S(k)$  functions such that  $S_{\text{corrected}}(k) = S_{\text{observed}}(k) / S_{\text{response}}(k)$ . We measured  $S_{\text{response}}$  for our system using fluorescent particles with diameters well below optical resolution (150 nm) and approximated it by a Gaussian with  $\sigma = 210$  nm. Correlation lengths,  $\xi$ , and osmotic compressibilities,  $\chi$ , were extracted from time-averaged, corrected  $S(k)$  curves by fit-

ting to the functional form  $S(k) = \chi / (1 + (\xi k)^2)^{7/4}$  (11). Errors in the fitting parameters  $\xi$  and  $\chi$  were determined directly from the covariance matrix at the best fit solution.

Correlation times are approximated by evaluating the time autocorrelation function of 750 nm by 750 nm square patches on the vesicle surface, averaging the curves obtained for all patches examined in a given vesicle, and fitting to  $e^{-Dt}$  as illustrated in Supplementary Figure S2. Square patches of 750 nm<sup>2</sup> were chosen because they are above the optical resolution of our images, and enough patches can be examined from a vesicle to obtain good statistics. The correlation times plotted in Figure 3, panel f, are the measured correlation time divided by the area probed (0.56  $\mu\text{m}^2$ ) to give  $D^{-1}$  with units of an inverse diffusion coefficient ( $\text{s}/\mu\text{m}^2$ ).

**Acknowledgment:** We thank B. Widom, J. Sethna, B. Stottrup, K. Gawrisch, and S. L. Keller for helpful conversations. SLV acknowledges a postdoctoral fellowship from the Cancer Research Institute. All research was supported by a grant from the National Institutes of Health (NIH AI18306).

**Supporting Information Available:** This material is free of charge via the Internet.

## REFERENCES

1. Simons, K., and Ikonen, E. (1997) Functional rafts in cell membranes, *Nature* **387**, 569–572.
2. Mayor, S., and Rao, M. (2004) Rafts: scale-dependent, active lipid organization at the cell surface, *Traffic* **5**, 231–240.
3. Hancock, J. F., and Parton, R. G. (2005) Ras plasma membrane signalling platforms, *Biochem. J.* **389**, 1–11.
4. Suzuki, K. G., Fujiwara, T. K., Sanematsu, F., Iino, R., Edidin, M., and Kusumi, A. (2007) GPI-anchored receptor clusters transiently recruit Lyn and G alpha for temporary cluster immobilization and Lyn activation: single-molecule tracking study 1, *J. Cell Biol.* **177**, 717–730.
5. Dietrich, C., Bagatolli, L. A., Volovyk, Z. N., Thompson, N. L., Levi, M., Jacobson, K., and Gratton, E. (2001) Lipid rafts reconstituted in model membranes, *Biophys. J.* **80**, 1417–1428.
6. Gidwani, A., Holowka, D., and Baird, B. (2001) Fluorescence anisotropy measurements of lipid order in plasma membranes and lipid rafts from RBL-2H3 mast cells, *Biochemistry* **40**, 12422–12429.
7. Ge, M., Gidwani, A., Brown, H. A., Holowka, D., Baird, B., and Freed, J. H. (2003) Ordered and disordered phases coexist in plasma membrane vesicles of RBL-2H3 mast cells. An ESR study, *Biophys. J.* **85**, 1278–1288.
8. Baumgart, T., Hammond, A. T., Sengupta, P., Hess, S. T., Holowka, D. A., Baird, B. A., and Webb, W. W. (2007) Large-scale fluid/fluid phase separation of proteins and lipids in giant plasma membrane vesicles, *Proc. Natl. Acad. Sci. U.S.A.* **104**, 3165–3170.
9. Sengupta, P., Holowka, D., and Baird, B. (2007) Fluorescence resonance energy transfer between lipid probes detects nanoscopic heterogeneity in the plasma membrane of live cells, *Biophys. J.* **92**, 3564–3574.
10. Swamy, M. J., Ciani, L., Ge, M., Smith, A. K., Holowka, D., Baird, B., and Freed, J. H. (2006) Coexisting domains in the plasma membranes of live cells characterized by spin-label ESR spectroscopy, *Biophys. J.* **90**, 4452–4465.
11. Fisher, M. E. (1964) Correlation functions and the critical region of simple fluids, *J. Math. Phys.* **5**, 944–962.
12. Sengers, J. V., and Levelt Sengers, J. M. H. (1986) Thermodynamic behavior of fluids near the critical point, *Annu. Rev. Phys. Chem.* **37**, 189–222.
13. Widom, B. (1965) Surface tension and molecular correlations near a critical point, *J. Chem. Phys.* **43**, 3892–3897.
14. Onsager, L. (1944) Crystal Statistics. I. A Two-Dimensional Model with an Order-Disorder Transition, *Phys. Rev.* **65**, 117–149.
15. Dunlavy, M. J., and Venus, D. (2005) Critical slowing down in the two-dimensional Ising model measured using ferromagnetic ultrathin films, *Phys Rev B* **71**, 144406.
16. Bechhoefer, J., Duval, J. L., Masson, L., Jerome, B., Homreich, R. M., and Pieranski, P. (1990) Critical Behavior in Anchoring Transitions of Nematic Liquid-Crystals, *Phys. Rev. Lett.* **64**, 1911–1914.
17. Veatch, S. L., Soubias, O., Keller, S. L., and Gawrisch, K. (2007) Critical fluctuations in domain-forming lipid mixtures, *Proc. Natl. Acad. Sci. U.S.A.* **104**, 17650–17655.
18. Honerkamp-Smith, A. R., Cicuta, P., Collins, M., Veatch, S. L., Schick, M., den Nijs, M., and Keller, S. L. (2008) Line tensions, correlation lengths, and critical exponents in lipid membranes near critical points, *Biophys. J.*, in press.
19. Widom, B. (1977) Structure and thermodynamics of interfaces, in *Statistical mechanics and statistical methods in theory and application* (Landman, U., Ed.), Plenum Press, New York.
20. Swinney, H. L., and Henry, D. L. (1973) Dynamics of fluids near the critical point: decay rate of order-parameter fluctuations, *Phys. Rev. A* **8**, 2586–2617.
21. Lacasse, M. D., Viñals, J., and Grant, M. (1993) Dynamic Monte Carlo renormalization-group method, *Phys. Rev. B* **47**, 5646–5652.
22. Wu, E. S., Tank, D. W., and Webb, W. W. (1982) Unconstrained lateral diffusion of concanavalin-a receptors on bulbous lymphocytes, *Proc. Natl. Acad. Sci. U.S.A.* **79**, 4962–4966.
23. Oradd, G., Westerman, P. W., and Lindblom, G. (2005) Lateral diffusion coefficients of separate lipid species in a ternary raft-forming bilayer: a Pfg-NMR multinuclear study, *Biophys. J.* **89**, 315–320.
24. Menon, A. K., Holowka, D., and Baird, B. (1984) Small oligomers of immunoglobulin E (IgE) cause large-scale clustering of IgE receptors on the surface of rat basophilic leukemia cells, *J. Cell Biol.* **98**, 577–583.
25. Tserkovnyak, Y., and Nelson, D. R. (2006) Conditions for extreme sensitivity of protein diffusion in membranes to cell environments, *Proc. Natl. Acad. Sci. U.S.A.* **103**, 15002–15007.

26. Collins, M. D., and Keller, S. L. (2008) Tuning lipid mixtures to induce or suppress domain formation across leaflets of unsupported asymmetric bilayers, *Proc. Natl. Acad. Sci. U.S.A.* **105**, 124–128.
27. Gheber, L. A., and Edidin, M. (1999) A model for membrane patchiness: lateral diffusion in the presence of barriers and vesicle traffic, *Biophys. J.* **77**, 3163–3175.
28. Veatch, S. L. (2007) From small fluctuations to large-scale phase separation: lateral organization in model membranes containing cholesterol, *Semin. Cell Dev. Biol.* **18**, 573–582.
29. Keller, S. L., Pitcher, W. H., Huestis, W. H., and McConnell, H. M. (1998) Red blood cell lipids form immiscible liquids, *Phys. Rev. Lett.* **81**, 5019–5022.
30. Hammond, A. T., Heberle, F. A., Baumgart, T., Holowka, D., Baird, B., and Feigenson, G. W. (2005) Crosslinking a lipid raft component triggers liquid ordered-liquid disordered phase separation in model plasma membranes, *Proc. Natl. Acad. Sci. U.S.A.* **102**, 6320–6325.
31. Liu, A. P., and Fletcher, D. A. (2006) Actin polymerization serves as a membrane domain switch in model lipid bilayers, *Biophys. J.* **91**, 4064–4070.
32. Seul, M., and Sammon, M. J. (1990) Competing interactions and domain-shape instabilities in a monomolecular film at an air-water interface, *Phys. Rev. Lett.* **64**, 1903–1906.
33. Stottrup, B. L., Heussler, A. M., and Bibelnieks, T. A. (2007) Determination of line tension in lipid monolayers by fourier analysis of capillary waves, *J. Phys. Chem. B* **111**, 11091–11094.
34. Esposito, C., Tian, A., Melamed, S., Johnson, C., Tee, S. Y., and Baumgart, T. (2007) Flicker spectroscopy of thermal lipid bilayer domain boundary fluctuations, *Biophys. J.* **93**, 3169–3181.
35. Baumgart, T., Hammond, A., Sengupta, P., Holowka, D., Baird, B., and Webb, W. W. (2006) Imaging of protein partitioning in plasma membranes with coexisting fluid phases, *Biophys. Soc. Meeting Abstr. Biophys. J. Suppl.* **20a**, Abstract, 758-Plat.